Available online at www.sciencedirect.com
ScienceDirect
Journal of Sound and Vibration 321 (2009) 254–269
JOURNAL OF SOUND AND VIBRATION
www.elsevier.com/locate/jsvi

An exact series solution for the transverse vibration of rectangular plates with general elastic boundary supports

W.L. Li[a,*], Xuefeng Zhang[a], Jingtao Du[b], Zhigang Liu[b]

[a]*Department of Mechanical Engineering, Wayne State University, 5050 Anthony Wayne Drive, Detroit, MI 48202, USA*
[b]*College of Power and Energy Engineering, Harbin Engineering University, Harbin 150001, PR China*

Received 3 March 2008; received in revised form 10 September 2008; accepted 18 September 2008
Handling Editor: S. Bolton
Available online 1 November 2008

Abstract

An analytical method is developed for the vibration analysis of rectangular plates with elastically restrained edges. The displacement solution is expressed as a two-dimensional Fourier series supplemented with several one-dimensional Fourier series. Mathematically, such a series expansion is capable of representing *any* function (including the exact displacement solution) whose third-order partial derivatives are (required to be) continuous over the area of the plate. Since the discontinuities (or jumps) potentially related to the partial derivatives at the edges (when they are periodically extended onto the entire x–y plane as implied by a two-dimensional Fourier series expansion) have been explicitly "absorbed" by the supplementary terms, all the series expansions for up to the fourth-order derivatives can be directly obtained through term-by-term differentiations of the displacement series. Thus, an exact solution can be obtained by letting the series simultaneously satisfy the governing differential equation and the boundary conditions on a point-wise basis. Because the series solution has to be truncated numerically, the "exact solution" should be understood as *a solution with arbitrary precision*. Several numerical examples are presented to illustrate the excellent accuracy of the current solution. The proposed method can be directly extended to other more complicated boundary conditions involving non-uniform elastic restraints, point supports, partial supports, and their combinations.

1. Introduction

Transverse vibrations of rectangular plates with various boundary conditions have been extensively studied in the literature, as comprehensively reviewed by Leissa [1]. While exact solutions are available for plates that are simply supported along at least one pair of opposite edges, it has been widely accepted that there exists no exact solution for other more general boundary conditions. Accordingly, a variety of approximate or numerical solution techniques have been employed to solve plate problems under different boundary conditions. Rayleigh–Ritz method is one of the most widely used techniques for obtaining an approximate solution. When the Rayleigh–Ritz method is employed in solving plate problems, the displacement function is often expressed in terms of characteristic functions obtained for beams with similar boundary conditions [2–6].

*Corresponding author. Tel.: +1 313 577 3875.
E-mail address: wli@wayne.edu (W.L. Li).

0022-460X/$ - see front matter © 2008 Elsevier Ltd. All rights reserved.
doi:10.1016/j.jsv.2008.09.035

Nomenclature

a	plate dimension in x-direction
b	plate dimension in y-direction
h	plate thickness
ρ	mass density
E	Young's modulus
v	Poisson's ratio
D	flexural rigidity ($= Eh^3/(12(1-v^2))$)
$w(x,y)$	flexural displacement
M, N	Fourier series truncation number in, respectively, x- and y-directions
m	Fourier series index in x-direction ($= 0, 1, \ldots, M-1$)
n	Fourier series index in y-direction ($= 0, 1, \ldots, N-1$)
p	rearrange index number ($= nM+m$)
l	index in the special functions and single Fourier series ($= 1, 2, 3, 4$)
r	aspect ratio ($= a/b$)
δ_{mn}	Kronecker delta function
λ_{am}	$m\pi/a$
λ_{bn}	$n\pi/a$
Ω	dimensionless frequency parameter ($= \omega a^2\sqrt{\rho h/D}$)
ω	angular frequency
$\mathbf{K}$	stiffness matrix
$\mathbf{M}$	mass matrix
A_{mn}	double Fourier series coefficients
c_m^l, d_n^l	single Fourier series coefficients
k_{x0}, k_{xa}	translational stiffnesses at, respectively, $x = 0$ and $x = a$
k_{y0}, k_{yb}	translational stiffnesses at, respectively, $y = 0$ and $y = b$
K_{x0}, K_{xa}	rotational stiffnesses at, respectively, $x = 0$ and $x = a$
K_{y0}, K_{yb}	rotational stiffnesses at, respectively, $y = 0$ and $y = b$
M_x, M_y	bending moment
M_{xy}	twisting moment
Q_x, Q_y	shear forces

Although the characteristic functions are well known in the form of trigonometric and hyperbolic functions, they are explicitly dependent on the boundary conditions. Consequently, a specific set of characteristic functions for each type of boundary conditions is required. However, even considering only the four simplest homogeneous cases (i.e., simply supported, clamped, free, and guided), one realizes that they can be combined into 55 different types of boundary conditions for a rectangular plate. Thus, the use of beam functions will lead to at least a very tedious solution process, not to mention potential difficulties associated with numerical instability of higher-order characteristic functions. These issues and concerns will become more remarkable for plates with elastically restrained edges.

Instead of the beam functions, one can also use other forms of admissible functions such as simple or orthogonal polynomials, trigonometric functions, and their combinations [7–16]. When the admissible functions do not form a complete set, the accuracy and convergence of the corresponding solution cannot be easily estimated. A well-known problem with use of complete (orthogonal) polynomials is that the higher-order polynomials tend to become numerically unstable due to the computer round-off errors. This numerical difficulty can be avoided by using trigonometric functions [11–13] or combinations of trigonometric functions and lower-order polynomials [14–16]. Although it has become a "standard" practice to express the plate displacement function as a series expansion of beam functions, there is no guarantee mathematically that such a representation will actually converge to the true solution because of the difference between the beam and plate boundary conditions. While the mathematical consequence of such a treatment is not readily assessed, its practical implication becomes immediately clear when a non-uniform boundary condition is specified along an edge; i.e., a *similar* boundary condition cannot be readily defined for determining the *appropriate* beam functions.

A systematic superposition method has been proposed by Gorman [17–20] for solving plate problems under various boundary conditions. In the superposition method a general boundary condition is decomposed into a number of "simple" boundary conditions for which analytical solutions exist or can be easily derived. In essence, the solutions obtained by the superposition method are exact since the governing differential equation is exactly satisfied throughout the entire domain of the plate. This technique, however, requires a good understanding and skillful decomposition of the original problems. In addition, the solution process essentially needs to be customized for each kind of boundary conditions, which may not be a small challenge

in view of the variety of possible boundary conditions encountered in practice. Hurlebaus et al. [21] proposed a Fourier cosine series solution for calculating the eigenfrequencies and mode shapes for a (composite) plate with completely free edges. The exactness of this solution was questioned by Rosales and Filipich [22]. In particular, they insisted that when uniform convergence of the essential functions (which include the slopes in the plate problem) could not be ensured, there was the probability that eigenvalues would converge to an approximate value, or even worse, jump to different eigenvalues (i.e., the loss of eigenvalues). In an earlier paper [23], they developed a variational method, the so-called whole-element method (WEM), to calculate the natural frequencies of a free rectangular plate. The displacement solution was expressed in the form of sine series plus a few complementary terms, and the solution was obtained as an extremizing sequence corresponding to the stationarity condition for a functional defined over the domain of the plate. Probably because of the free boundary condition specified along each edge, the functional they used did not contain any boundary variable or involve any boundary integral. Mathematical proofs were presented in their paper regarding the exactness of eigenvalues and uniform convergence of essential functions.

It is not clear whether or not the series solutions derived in Refs. [21,23] can be extended to boundary conditions than the completely free case. Although these series solutions were claimed to be able to exactly calculate eigenfrequencies, mode shapes, and even slopes, they may not automatically become an exact solution in the classical sense because a classical solution will have to be sufficiently smooth; i.e., the third-order derivatives will have to be continuous, and the fourth-order derivatives will have to exist everywhere on the plate. For example, if the moments and shear forces cannot be assured to be exact throughout the plate and along the edges (when they are not completely free), it may not be possible to ascertain that eigenfrequencies and mode shapes can be calculated exactly or with an arbitrary precision. These questions or concerns can all be circumvented by the proposed solution, which is also expressed in the form of series expansions. It is, however, substantially different from the aforementioned series solutions in that it can be differentiated term-by-term to obtain other useful quantities (such as, slopes, moments, and shear forces) at any point on the plate, and hence it can be directly substituted in the governing equation and boundary conditions to solve for unknown expansion coefficients in an exact manner. This work represents an extension of the solution method previously developed for analyzing vibrations of beams [24], and in-plane vibrations of plates [25]. In comparison with the solutions for in-plane vibrations, the current one will have to include more supplementary terms to improve smoothness (and hence rate of convergence) of the displacement function and to account for potential discontinuities with higher-order derivatives along edges when they are periodically extended onto the entire x–y plane. A new set of supplementary functions is provided in the form of trigonometric functions, which are essentially unaffected by differential operations and can avoid the possibility of nullifying a boundary condition. The mathematical and numerical advantages of the current solution method will become obvious from the following discussions.

2. Vibration of a rectangular plate

Consider a rectangular plate elastically restrained along any edge(s), as shown in Fig. 1. The governing differential equation for free vibration of a plate is given by

$$D\nabla^4 w(x,y) - \rho h\omega^2 w(x,y) = 0, \tag{1}$$

where $\nabla^4 = \partial^4/\partial x^4 + 2\partial^4/\partial x^2\partial y^2 + \partial^4/\partial y^4$, $w(x,y)$ is the flexural displacement, ω the angular frequency, and D, ρ, and h are, respectively, the flexural rigidity, the mass density, and the thickness of the plate.

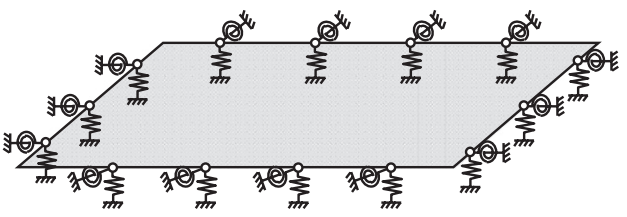

Fig. 1. A rectangular plate elastically restrained along all edges.

In terms of flexural displacements, the bending and twisting moments, and transverse shearing forces can be expressed as

$$M_x = -D\left(\frac{\partial^2 w}{\partial x^2} + v\frac{\partial^2 w}{\partial y^2}\right), \tag{2}$$

$$M_y = -D\left(\frac{\partial^2 w}{\partial y^2} + v\frac{\partial^2 w}{\partial x^2}\right), \tag{3}$$

$$M_{xy} = -D(1-v)\frac{\partial^2 w}{\partial x\,\partial y}, \tag{4}$$

$$Q_x = -D\frac{\partial}{\partial x}(\nabla^2 w) + \frac{\partial M_{xy}}{\partial y} = -D\left(\frac{\partial^3 w}{\partial x^3} + (2-v)\frac{\partial^3 w}{\partial x\,\partial y^2}\right), \tag{5}$$

and

$$Q_y = -D\frac{\partial}{\partial y}(\nabla^2 w) + \frac{\partial M_{xy}}{\partial x} = -D\left(\frac{\partial^3 w}{\partial y^3} + (2-v)\frac{\partial^3 w}{\partial x^2\,\partial y}\right). \tag{6}$$

The boundary conditions for an elastically restrained rectangular plate are as follows:

$$k_{x0}w = Q_x, \quad K_{x0}\,\partial w/\partial x = -M_x, \quad \text{at} \quad x = 0, \tag{7,8}$$

$$k_{xa}w = -Q_x, \quad K_{xa}\,\partial w/\partial x = M_x, \quad \text{at} \quad x = a, \tag{9,10}$$

$$k_{y0}w = Q_y, \quad K_{y0}\,\partial w/\partial y = -M_y, \quad \text{at} \quad y = 0, \tag{11,12}$$

and

$$k_{yb}w = -Q_y, \quad K_{yb}\,\partial w/\partial y = M_y, \quad \text{at} \quad y = b, \tag{13,14}$$

where k_{x0} and k_{xa} (k_{y0} and k_{yb}) are the linear spring constants, and K_{x0} and K_{xa} (K_{y0} and K_{yb}) the rotational spring constants at $x = 0$ and $x = a$ ($y = 0$ and $y = b$), respectively. Eqs. (7)–(14) represent a set of general boundary conditions from which, for example, all the classical homogeneous boundary conditions can be directly obtained by accordingly setting the spring constants to be extremely large or small.

Substitution of Eqs. (2)–(6) into (7)–(14) leads to

$$k_{x0}w(x,y) = -D\left(\frac{\partial^3 w}{\partial x^3} + (2-v)\frac{\partial^3 w}{\partial x\,\partial y^2})\right), \quad K_{x0}\frac{\partial w}{\partial x} = D\left(\frac{\partial^2 w}{\partial x^2} + v\frac{\partial^2 w}{\partial y^2}\right) \quad \text{at} \quad x = 0, \tag{15,16}$$

$$k_{xa}w(x,y) = D\left(\frac{\partial^3 w}{\partial x^3} + (2-v)\frac{\partial^3 w}{\partial x\,\partial y^2})\right), \quad K_{xa}\frac{\partial w}{\partial x} = -D\left(\frac{\partial^2 w}{\partial x^2} + v\frac{\partial^2 w}{\partial y^2}\right) \quad \text{at} \quad x = a, \tag{17,18}$$

$$k_{y0}w(x,y) = -D\left(\frac{\partial^3 w}{\partial y^3} + (2-v)\frac{\partial^3 w}{\partial x^2\,\partial y}\right), \quad K_{y0}\frac{\partial w}{\partial y} = D\left(\frac{\partial^2 w}{\partial y^2} + v\frac{\partial^2 w}{\partial x^2}\right) \quad \text{at} \quad y = 0, \tag{19,20}$$

$$k_{yb}w(x,y) = D\left(\frac{\partial^3 w}{\partial y^3} + (2-v)\frac{\partial^3 w}{\partial x^2\,\partial y}\right) \quad \text{and} \quad K_{yb}\frac{\partial w}{\partial y} = -D\left(\frac{\partial^2 w}{\partial y^2} + v\frac{\partial^2 w}{\partial x^2}\right) \quad \text{at} \quad y = b. \tag{21,22}$$

An exact solution is widely considered unavailable for plates under such a set of general boundary conditions. As a consequence, the Rayleigh–Ritz method or some other methods have been usually used to find an approximate solution.

In this study, the displacement function will be sought in the form of series expansions as

$$w(x,y) = \sum_{m=0}^{\infty}\sum_{n=0}^{\infty} A_{mn}\cos\lambda_{am}x\cos\lambda_{bn}y + \sum_{l=1}^{4}\left(\xi_b^l(y)\sum_{m=0}^{\infty}c_m^l\cos\lambda_{am}x + \xi_a^l(x)\sum_{n=0}^{\infty}d_n^l\cos\lambda_{bn}y\right), \tag{23}$$

where $\lambda_{am} = m\pi/a$, $\lambda_{bn} = n\pi/b$, and $\xi_a^l(x)$ (or $\xi_b^l(y)$) represent a set of closed-form sufficiently smooth functions defined over [0, a] (or [0, b]). The term "sufficiently smooth" implies that third-order derivatives of these functions exist and are continuous at any point on the plate. Such requirements can be readily satisfied by simple polynomials [14,24,25]. Theoretically, there are an infinite number of these supplementary functions. However, one needs to ensure that the selected functions will not nullify any of the boundary conditions. As mentioned earlier, these functions are introduced specifically to take care of possible discontinuities with first and third derivatives at each edge. In the subsequent solution phase, however, the expansion coefficients will have to be directly solved from the governing equations and the boundary conditions. Thus, the selected supplementary functions should not interfere with this process in any way. To better understand it, let us consider, for example, the boundary condition, Eq. (16). If the supplementary functions and their second derivatives (with respect to x) all vanish at $x = 0$, then this boundary condition will be mathematically nullified for $K_{x0} = 0$. In other words, the resulting coefficient matrix will become singular for $K_{x0} = 0$. Similar situations can occur at other edges. With this in mind, the supplementary functions will be here chosen in the form of trigonometric functions, which are essentially unaffected by differential operations:

$$\xi_a^1(x) = \frac{9a}{4\pi}\sin\left(\frac{\pi x}{2a}\right) - \frac{a}{12\pi}\sin\left(\frac{3\pi x}{2a}\right), \quad \xi_a^2(x) = -\frac{9a}{4\pi}\cos\left(\frac{\pi x}{2a}\right) - \frac{a}{12\pi}\cos\left(\frac{3\pi x}{2a}\right), \tag{24, 25}$$

$$\xi_a^3(x) = \frac{a^3}{\pi^3}\sin\left(\frac{\pi x}{2a}\right) - \frac{a^3}{3\pi^3}\sin\left(\frac{3\pi x}{2a}\right), \quad \xi_a^4(x) = -\frac{a^3}{\pi^3}\cos\left(\frac{\pi x}{2a}\right) - \frac{a^3}{3\pi^3}\cos\left(\frac{3\pi x}{2a}\right). \tag{26, 27}$$

It is easy to verify that $\xi_a^{1'}(0) = \xi_a^{2'}(a) = \xi_a^{3'''}(0) = \xi_a^{4'''}(a) = 1$, and all the other first and third derivatives are identically equal to zero at the edges. These conditions are not necessary, but make it easier to understand the meanings of the one-dimensional Fourier series expansions: each of them represents either the first or the third derivative of the displacement function at one of the edges. By doing such, the two-dimensional series will be "forced" to represent a residual displacement function that has, at least, three continuous derivatives in both x- and y-directions.

It can be proven mathematically that the series expansion given in Eq. (23) is able to expand and uniformly converge to *any* function $f(x,y) \in \mathbb{C}^3$ for $\forall(x,\ y) \in D$: ([0, a]$\otimes$[0, b]). Also, this series can be simply differentiated, through term-by-term, to obtain uniformly convergent series expansions for up to the fourth-order derivatives. Mathematically, an exact displacement (or classical) solution is a *particular* function $w(x,y) \in \mathbb{C}^3$ for $\forall(x,\ y) \in D$ that satisfies the governing equation at *every* field point and the boundary conditions at *every* boundary point. Thus, the remaining task for seeking an exact displacement solution will simply involve finding a set of expansion coefficients to ensure the governing equation and the boundary conditions to be satisfied by the current series solution *exactly on a point-wise basis*.

When a plate problem is amenable to the separation of variables, an exact solution is usually expressed as a series expansion where *each* term will simultaneously satisfy the *homogeneous* governing equation and the boundary conditions. However, in determining the response to an applied load, it should not matter whether the governing equation or a boundary condition is satisfied *individually* by each term or *globally* by the whole series. Take a simply supported plate as an example. A sine function will be able to exactly satisfy the characteristic equation and boundary conditions at each edge. Then the exact solution is often understood as a simple Fourier series, which may also be interpreted as a modal expansion. To calculate the vibrational response, however, the governing equation will usually include two more terms to account for the damping effect and the loading condition, and the solution (the expansion coefficients) is obtained by equating the like terms on both sides (of course, it must be explicitly assumed that the forcing function can also be expanded into a sine series). In other words, the governing equation is actually satisfied globally by the series, rather than individually by each term. Since in real calculations a series solution will have to be truncated somewhere according to a pre-determined error bound, an *exact* solution really implies that the results can be obtained to *any desired degree of accuracy*. This characterization applies equally to the current solution as described below. The only procedural difference between the classical solution and the proposed one is that the boundary conditions there are automatically satisfied by each term, and the expansion coefficients are only required to satisfy the governing equation; in comparison, the expansion coefficients in the current solution will have to explicitly satisfy both the governing equation and the boundary conditions. This distinction probably will not

have mathematical significance in regard to the convergence and accuracy of the solution although a pre-satisfaction of the boundary conditions or governing equation by each of the expansion terms may result in a reduction of the computing effort.

In what follows, our attention will be directed to solving the unknown expansion coefficients by letting the assumed solution satisfy both the governing equation and the boundary conditions.

Substituting the displacement expression, Eq. (23), into the boundary condition, Eq. (15), results in

$$k_{x0}\left(\sum_{m=0}^{\infty}\sum_{n=0}^{\infty}A_{mn}\cos\lambda_{bn}y+\sum_{l=1}^{4}\left(\xi_b^l(y)\sum_{m=0}^{\infty}c_m^l+\xi_a^l(0)\sum_{n=0}^{\infty}d_n^l\cos\lambda_{bn}y\right)\right)$$
$$=-D\left((2-v)\sum_{n=0}^{\infty}-\lambda_{bn}^2d_n^1\cos\lambda_{bn}y+\sum_{n=0}^{\infty}d_n^3\cos\lambda_{bn}y\right). \tag{28}$$

It is seen that in the above equation all the terms, except for the second one, are in the form of cosine series expansion in y-direction. So it is natural to also expand $\xi_b^l(y)$ into a cosine series, i.e., $\xi_b^l(y)=\sum_{n=0}^{\infty}\beta_n^l\cos\lambda_{bn}y$. By equating the coefficients for the like terms on both sides, the following equations can be derived:

$$\frac{k_{x0}}{D}\sum_{l=1}^{4}\left(\beta_n^l\sum_{m=0}^{\infty}c_m^l+\xi_a^l(0)d_n^l\right)+(2-v)(-\lambda_{bn}^2)d_n^1+d_n^3=-\frac{k_{x0}}{D}\sum_{m=0}^{\infty}A_{mn}\quad(n=0,1,2\ldots\infty). \tag{29}$$

Three similar equations can be directly obtained from Eqs. (17)–(19):

$$\sum_{l=1}^{4}\sum_{m=0}^{\infty}[-\lambda_{am}^2\beta_n^l+v\bar{\beta}_n^l]c_m^l+\sum_{l=1}^{4}[\xi''^l{}_a(0)-v\lambda_{bn}^2\xi_a^l(0)]d_n^l-\frac{K_{x0}}{D}d_n^1=\sum_{m=0}^{\infty}(\lambda_{am}^2+v\lambda_{bn}^2)A_{mn}$$
$$(n=0,1,2\ldots\infty,\ x=0), \tag{30}$$

$$\frac{k_{xa}}{D}\sum_{l=1}^{4}\left(\beta_n^l\sum_{m=0}^{\infty}(-1)^mc_m^l+\xi_a^l(a)d_n^l\right)+(2-v)\lambda_{bn}^2d_n^2-d_n^4=\frac{k_{xa}}{D}\sum_{m=0}^{\infty}(-1)^{m+1}A_{mn}$$
$$(n=0,1,2\ldots\infty,\ x=a), \tag{31}$$

and

$$\sum_{l=1}^{4}\sum_{m=0}^{\infty}(-1)^m(v\bar{\beta}_n^l-\lambda_{am}^2\beta_n^l)c_m^l+\sum_{l=1}^{4}[\xi''^l{}_a(a)-v\lambda_{bn}^2\xi_a^l(a)]d_n^l+\frac{K_{xa}}{D}d_n^2=\sum_{m=0}^{\infty}(-1)^m(\lambda_{am}^2+v\lambda_{bn}^2)A_{mn}$$
$$(n=0,1,2\ldots\infty,\ x=a), \tag{32}$$

where $\xi_b^{l''}(y)=\sum_{n=0}^{\infty}\bar{\beta}_n^l\cos\lambda_{bn}y$, and the new symbols β_n^l and $\bar{\beta}_n^l$ in the above equations are defined in Appendix A.

These equations indicate that the unknown coefficients in the two- and one-dimensional series expansions are not independent. They have to explicitly comply with the constraint conditions, Eqs. (29)–(32). Four more constraint equations corresponding to the boundary conditions at the remaining two edges can be readily written out by replacing the variable m, β_n^l, $\bar{\beta}_n^l$, a, and x with n, α_m^l, $\bar{\alpha}_m^l$, b, and y, respectively. It now becomes clear that the satisfaction of these constraint equations by the expansion coefficients is equivalent to an *exact* satisfaction of all the boundary conditions (by the displacement function) *on a point-wise basis*.

The constraint equations can be rewritten in a matrix form as

$$\mathbf{Hp}=\mathbf{Qa}, \tag{33}$$

where $\mathbf{p}=[c_1^1,c_2^1\ldots c_M^1,c_1^2,c_2^2\ldots c_M^2,\ldots,c_1^4,c_2^4\ldots c_M^4,d_1^1,d_2^1\ldots d_N^1,d_1^2,d_2^2,\ldots,d_1^4,d_2^4\ldots d_N^4]^{\mathrm{T}}$ and $\mathbf{a}=[A_{01},A_{11}\ldots A_{M1}\ldots A_{02},A_{12}\ldots A_{M2}\ldots A_{0N},A_{1N}\ldots A_{MN}]^{\mathrm{T}}$. The new matrices $\mathbf{H}$ and $\mathbf{Q}$ are defined in Appendix B. In Eq. (33), it is assumed that all the series expansions are truncated to $m=M$ and $n=N$ for the sake of numerical implementation.

Eq. (33) represents a set of $4(M+N)$ equations against a total of $4(M+N)+M\times N$ unknown expansion coefficients. Thus, additional $M\times N$ equations will have to be provided to solve for the expansion coefficients.

By substituting Eq. (23) into the governing differential equation, one is able to get

$$\sum_{m=0}^{\infty}\sum_{n=0}^{\infty}(\lambda_{am}^4+\lambda_{bn}^4+2\lambda_{am}^2\lambda_{bn}^2)A_{mn}\cos\lambda_{am}x\cos\lambda_{bn}y + \sum_{l=1}^{4}\sum_{m=0}^{\infty}(\xi_b^l(y)\lambda_{am}^4-2\lambda_{am}^2\xi''^l{}_b(y)+\xi_b^{(4)l}(y))c_m^l\cos\lambda_{am}x + \sum_{l=1}^{4}\sum_{n=0}^{\infty}(\xi_a^l(x)\lambda_{bn}^4-2\lambda_{bn}^2\xi''^l{}_a(x)+\xi_a^{(4)l}(x))d_n^l\cos\lambda_{bn}y - \frac{\rho h\omega^2}{D}\left[\sum_{m=0}^{\infty}\sum_{n=0}^{\infty}A_{mn}\cos\lambda_{am}x\cos\lambda_{bn}y+\sum_{l=1}^{4}\left(\xi_b^l(y)\sum_{m=0}^{\infty}c_m^l\cos\lambda_{am}x+\xi_a^l(x)\sum_{n=0}^{\infty}d_n^l\cos\lambda_{bn}y\right)\right]=0. \quad (34)$$

Again, after all the non-cosine functions in the above equation are expanded into Fourier cosine series, $\xi_b^{l(4)}(y)=\sum_{n=0}^{\infty}\bar{\bar{\beta}}_n^l\cos\lambda_{bn}y$ the following equations can be obtained by comparing the like terms on both sides:

$$(\lambda_{am}^4+\lambda_{bn}^4+2\lambda_{am}^2\lambda_{bn}^2)A_{mn}+\sum_{l=1}^{4}(\beta_n^l\lambda_{am}^4-2\lambda_{am}^2\bar{\beta}_n^l+\bar{\bar{\beta}}_n^l)c_m^l+\sum_{l=1}^{4}(\alpha_m^l\lambda_{bn}^4-2\lambda_{bn}^2\bar{\alpha}_m^l+\bar{\bar{\alpha}}_m^l)d_n^l - \frac{\rho h\omega^2}{D}\left[A_{mn}+\sum_{l=1}^{4}(\beta_n^l c_m^l+\alpha_m^l d_n^l)\right]=0, \quad (35)$$

where $m=0,1,\ldots,M-1$ and $n=0,1,\ldots,N-1$. It can be further written in a matrix form as

$$(\tilde{\mathbf{K}}\,\mathbf{a}+\mathbf{B}\mathbf{p})-\frac{\rho h\omega^2}{D}(\tilde{\mathbf{M}}\,\mathbf{a}+\mathbf{F}\mathbf{p})=0. \quad (36)$$

The coefficient matrices in the above equation are defined in Appendix C.

Obviously, Eqs. (33) and (36) cannot be directly combined together to form a characteristic equation of the coefficient vectors **a** and **p** because the assembled mass matrix will become singular. By following the approach traditionally used for determining an eigenvalue, one may first solve Eq. (36) for **a** in terms of **p**. Substituting the result into the boundary conditions, Eq. (33), will lead to a set of homogeneous equations. The eigenvalues can then be obtained as the roots of a nonlinear function that is defined as the determinant of the coefficient matrix. Such an approach is numerically not preferable because of the well-known difficulties and concerns associated with solving a highly nonlinear equation. Instead, Eq. (33) will be used here to eliminate the vector **p** from Eq. (36), resulting in

$$\left(\mathbf{K}-\frac{\rho h\omega^2}{D}\mathbf{M}\right)\mathbf{a}=0, \quad (37)$$

where $\mathbf{K}=(\tilde{\mathbf{K}}+\mathbf{B}\mathbf{H}^{-1}\mathbf{Q})$ and $\mathbf{M}=(\tilde{\mathbf{M}}+\mathbf{F}\mathbf{H}^{-1}\mathbf{Q})$. Eq. (37) represents a standard matrix characteristic equation from which all the eigenpairs can be easily determined. Once the eigenvector **a** is determined for a given eigenvalue, the corresponding vector **p** can be calculated directly using Eq. (33). Subsequently, the mode shapes can be constructed by substituting **a** and **p** in Eq. (23).

Although this study is focused on free vibrations of an elastically restrained plate, forced vibrations can also be determined by simply adding a load vector to the right side of Eq. (37). It should be noted that the elements of the load vector represent the Fourier coefficients of the forcing function when it is expanded into a cosine series over the plate area.

3. Results and discussion

Several examples involving various boundary conditions will be discussed in this section. First, consider a plate fully clamped along all four edges. A clamped edge can be viewed as a special case when the stiffness constants for the (translational and rotational) springs become infinitely large (which is represented by a very large number, 5.0×10^7, in the actual calculations). In Table 1, the first six frequency parameters,

$\Omega = \omega a^2\sqrt{\rho h/D}$, are given for the clamped plates with different aspect ratios. The calculated frequencies show an excellent agreement with those previously given in Refs. [1,16]. As mentioned earlier, the series expansion, Eq. (23), will have to be truncated in numerical calculations. Specifically, the frequency parameters in Table 1 are determined by truncating the series to $M = N = 20$. To examine the convergence of the solution, Table 2 compares the frequencies (for $b/a = 1$) calculated by using different number of terms in the series expansion. It is shown that the results converge at $M = N = 17$ for the given five-digit precision. The excellent numerical stability of the solution is also evident. For consistency, the displacement expansion will be simply truncated to $M = N = 20$ in all the subsequent calculations.

The next example is about a plate which is clamped at $x = 0$ and free at all other edges (C–F–F–F). The free-edge condition is easily created by setting the stiffness constants for both springs equal to zero. This problem has been extensively studied both numerically and experimentally. The first six frequency parameters are presented in Table 3. The upper bound for frequency parameter was calculated using the Rayleigh–Ritz method by taking the first 50 admissible products of beam functions [1]. The finite-element method results were obtained from a model consisting of 300 linear rectangular elements along each edge. Two more classical cases (S–S–F–F and C–S–S–F) were also considered, and the corresponding frequency parameters are listed in Tables 4 and 5, respectively. For a simply supported edge, the stiffness for the transverse spring is infinitely

Table 1
Frequency parameters, $\Omega = \omega a^2\sqrt{\rho h/D}$, for C–C–C–C rectangular plates with different aspect ratios

$r = a/b$	$\Omega = \omega a^2\sqrt{\rho h/D}$					
	1	2	3	4	5	6
1.0	35.985	73.393	73.393	108.21	131.58	132.20
	35.986[a]	73.395	73.395	108.22	131.58	132.21
	35.985[b]	73.394	73.394	108.22	131.58	132.20
	35.985[c]	73.392	73.392	108.21	131.58	132.20
1.5	60.761	93.832	148.78	149.67	179.56	226.82
2.0	98.309	127.30	179.07	253.31	255.92	284.29
2.5	147.77	173.79	221.35	291.68	384.32	394.23
	147.8[a]	173.8	221.4	291.7	384.4	394.3
3.0	208.76	232.72	276.65	342.81	431.64	542.67
3.5	281.11	303.63	344.68	406.93	491.65	598.94
4.0	364.74	386.23	425.04	483.89	564.60	667.85

[a]Results from Ref. [16].
[b]Results from page 66 of Ref. [1].
[c]Results from FEM with 300×300 elements.

Table 2
Frequency parameters, $\Omega = \omega a^2\sqrt{\rho h/D}$, for a C–C–C–C square plate with different truncate numbers

$M = N$	$\Omega = \omega a^2\sqrt{\rho h/D}$					
	1	2	3	4	5	6
13	35.985	73.390	73.390	108.20	131.57	132.20
14	35.985	73.391	73.391	108.21	131.57	132.20
15	35.985	73.392	73.392	108.21	131.58	132.20
16	35.985	73.392	73.392	108.21	131.58	132.20
17	35.985	73.393	73.393	108.21	131.58	132.20
18	35.985	73.393	73.393	108.21	131.58	132.20
19	35.985	73.393	73.393	108.21	131.58	132.20
20	35.985	73.393	73.393	108.21	131.58	132.20

Table 3
Frequency parameters, $\Omega = \omega a^2\sqrt{\rho h/D}$, for C–F–F–F rectangular plate with different aspect ratios

$r = a/b$	$\Omega = \omega a^2\sqrt{\rho h/D}$					
	1	2	3	4	5	6
1.0	3.470	8.504	21.279	27.201	30.948	54.185
	3.430[a]		20.874	26.501		51.502
	3.482[b]		21.367	27.278		54.301
	3.471[c]	8.506	21.283	27.199	30.953	54.179
1.5	3.453	11.654	21.463	39.319	53.544	61.606
2.0	3.439	14.800	21.430	48.171	60.143	92.507
2.5	3.427	17.96	21.392	57.209	60.115	105.92
	3.428[c]	17.962	21.397	57.216	60.130	105.93
3.0	3.418	21.135	21.358	60.010	66.365	118.02
3.5	3.411	21.328	24.320	59.905	75.611	117.86
4.0	3.405	21.302	27.513	59.810	84.929	117.67

[a]Results from page 80 of Ref. [1] for lower bounds.
[b]Results from page 80 of Ref. [1] for upper bounds.
[c]Results from FEM with 300×300 elements.

Table 4
Frequency parameters, $\Omega = \omega a^2\sqrt{\rho h/D}$, for S–S–F–F rectangular plate with different aspect ratios

$r = a/b$	$\Omega = \omega a^2\sqrt{\rho h/D}$					
	1	2	3	4	5	6
1.0	3.370	17.321	19.293	38.203	51.032	53.497
	3.369[a]	17.41	19.37	38.30	51.35	53.74
	3.367[b]	17.316	19.293	38.210	51.034	53.484
1.5	5.023	21.458	37.527	55.220	60.726	99.107
2.0	6.644	25.370	58.739	65.183	89.084	113.17
2.5	8.244	29.559	64.457	98.681	117.76	125.62
	8.251[a]	29.65	64.77	99.24	118.3	126.1
	8.247[b]	29.564	64.468	98.679	117.78	125.61
3.0	9.850	33.903	70.245	123.48	141.64	167.65
3.5	11.442	38.336	76.443	130.80	189.99	204.62
4.0	13.037	42.835	82.962	138.39	211.48	248.87

[a]Results from Ref. [16].
[b]Results from FEM with 300×300 elements.

large and the stiffness for the rotational spring is set to zero. In both cases, the current results match well with the finite-element method data, and show a noticeable improvement over the results previously given in Ref. [16], which were obtained using the Rayleigh–Ritz method based on the products of beam functions.

The above examples are presented as special cases of elastically restrained plates. It is shown that the frequency parameters for classical homogeneous boundary conditions can be accurately determined by modifying the stiffnesses of the restraining springs accordingly. It should be emphasized that unlike most existing techniques, the current method offers a unified solution for a variety of boundary conditions, including all the classical cases, and the modification of boundary conditions from one case to another is as simple as changing the material properties or plate dimensions.

Let us now consider a few more complicated problems in which plates are elastically restrained at an edge. The first one involves a simply supported square plate with a uniform elastic restraint against rotation along

Table 5
Frequency parameters, $\Omega = \omega a^2\sqrt{\rho h/D}$, for C–S–S–F rectangular plate with different aspect ratios

$r = a/b$	$\Omega = \omega a^2\sqrt{\rho h/D}$					
	1	2	3	4	5	6
1.0	16.785	31.115	51.392	64.016	67.549	101.21
	16.87[a]	31.14	51.64	64.03	67.64	101.2
	16.790[b]	31.110	51.393	64.017	67.534	101.10
1.5	18.463	50.409	53.453	88.682	107.65	126.05
2.0	20.577	56.265	77.316	110.69	117.24	175.77
2.5	22.997	59.705	111.90	114.54	153.06	188.54
	23.07[a]	59.97	111.9	115.1	153.1	189.6
	23.003[b]	59.723	111.90	114.58	153.06	188.60
3.0	25.628	63.672	119.11	154.20	193.38	196.24
3.5	28.399	68.063	124.31	199.00	204.21	246.85
4.0	31.274	72.795	130.07	205.32	261.95	299.44

[a]Results from Ref. [16].
[b]Results from FEM with 300×300 elements.

Table 6
Frequency parameters, $\Omega = \omega a^2\sqrt{\rho h/D}$, for S–S–S–S square plate with uniform rotational restraint along edges

Ka/D	$\Omega = \omega a^2\sqrt{\rho h/D}$					
	1	2	3	4	5	6
1	21.500	51.187	51.187	80.816	100.58	100.59
	21.496[a]	51.184	51.184	80.818	100.58	100.58
10	28.501	60.215	60.215	90.808	111.19	111.41
	28.50[b]	60.22	60.22	90.81	111.2	111.4
	28.489[a]	60.196	60.196	90.790	111.16	111.39
100	34.671	70.780	70.780	104.45	127.02	127.61
	34.67[b]	70.78	70.78	104.5	127.0	127.6
	34.668[a]	70.771	70.771	104.44	127.01	127.59
1000	35.842	73.103	73.103	107.79	131.06	131.68
	35.842[a]	73.100	73.100	107.78	131.06	131.68

[a]Results from FEM with 300×300 elements.
[b]Results from Ref. [16].

each edge. The calculated frequency parameters are given in Table 6 together with those previously obtained using different models. These three sets of results match very well with each other. The second example concerns a cantilever square plate with the same elastic restraints added to $x = a$ and $y = b$. While the stiffness for the transverse spring is fixed to $ka^3/D = 10$, the rotational restraint will be considered at several different stiffness levels: $Ka/D = 1$, 10, 100, and 1000. The corresponding frequency parameters are shown in Table 7. It is seen that the first two frequencies are not very sensitive to the changes of rotational restraints, which is kind of anticipated from the similar trend for a cantilevered beam.

Last, consider a square plate elastically supported along all of its edges. The stiffnesses for the transverse and rotational restraints are chosen as $ka^3/D = 100$ and $Ka/D = 1000$, respectively. The frequency parameters are shown in Table 8 for plates with different aspect ratios from 1 to 4. Again, the current calculations compare well with the finite-element method results. Thus far, our attention has been focused on frequency parameters for different boundary conditions and aspect ratios. As a matter of fact, the eigenpairs (eigenfrequencies and eigenvectors) are simultaneously obtained from the characteristic equation, Eq. (37).

Table 7
Frequency parameters, $\Omega = \omega a^2\sqrt{\rho h/D}$, for C–F–F–F square plate with identical elastic restraints at $x = a$ and $y = b$, $ka^3/D = 10$ and $ka/D = 1, 10, 100, 1000$

Ka/D	$\Omega = \omega a^2\sqrt{\rho h/D}$					
	1	2	3	4	5	6
1	7.534	11.708	24.300	29.445	33.029	55.691
	7.518[a]	11.684	24.288	29.424	33.015	55.680
10	7.8104	12.317	28.408	32.72	35.924	58.791
	7.797[b]	12.299	28.397	32.697	35.909	58.772
100	7.899	12.597	30.218	34.537	37.574	61.077
	7.886[b]	12.581	30.215	34.525	37.569	61.069
1000	7.910	12.635	30.463	34.801	37.825	61.463
	7.897[b]	12.620	30.461	34.792	37.820	61.456

[a]Results from Ref. [16].
[b]Results from FEM with 300×300 elements.

Table 8
Frequency parameters, $\Omega = \omega a^2\sqrt{\rho h/D}$, for square plate with $ka^3/D = 100$ and $Ka/D = 1000$, respectively, at $x = 0, a$ and $y = 0, b$

$r = a/b$	$\Omega = \omega a^2\sqrt{\rho h/D}$					
	1	2	3	4	5	6
1.0	17.509	25.292	25.292	33.893	46.285	46.856
	17.474[a]	25.228	25.228	33.795	46.264	46.779
1.5	20.718	27.455	35.433	44.712	47.694	69.282
	20.664[a]	27.362	35.357	44.595	47.623	69.194
2.0	23.217	29.346	48.772	50.239	60.024	86.096
	23.151[a]	29.230	48.683	50.165	59.908	86.001
2.5	25.374	31.069	49.812	70.381	80.411	93.651
	25.298[a]	30.932	49.705	70.308	80.298	93.592
3.0	27.322	32.675	50.822	94.186	95.857	105.98
	27.238[a]	32.520	50.698	94.116	95.788	105.87
3.5	29.123	34.192	51.807	94.717	126.54	136.68
	29.038[a]	34.040	51.682	94.646	126.47	136.58
4.0	30.809	35.639	52.770	95.243	161.35	162.31
	30.710[a]	35.455	52.612	95.153	161.28	162.24

[a]Results from FEM with 300×300 elements.

For a given eigenfrequency, the corresponding eigenvector actually contains the expansion coefficients A_{mn}. In order to determine the mode shape, the expansion coefficients for one-dimensional Fourier series expansions also need to be calculated using Eq. (33). Once all the expansion coefficients are known, the mode shapes can be simply obtained from Eq. (23) in an analytical form. For example, plotted in Fig. 2 are the mode shapes that correspond to the six frequencies given in the first row of Table 8. Because the stiffnesses of the restraining springs are sufficiently large, the characteristics of the rigid body motions are effectively eliminated. Although

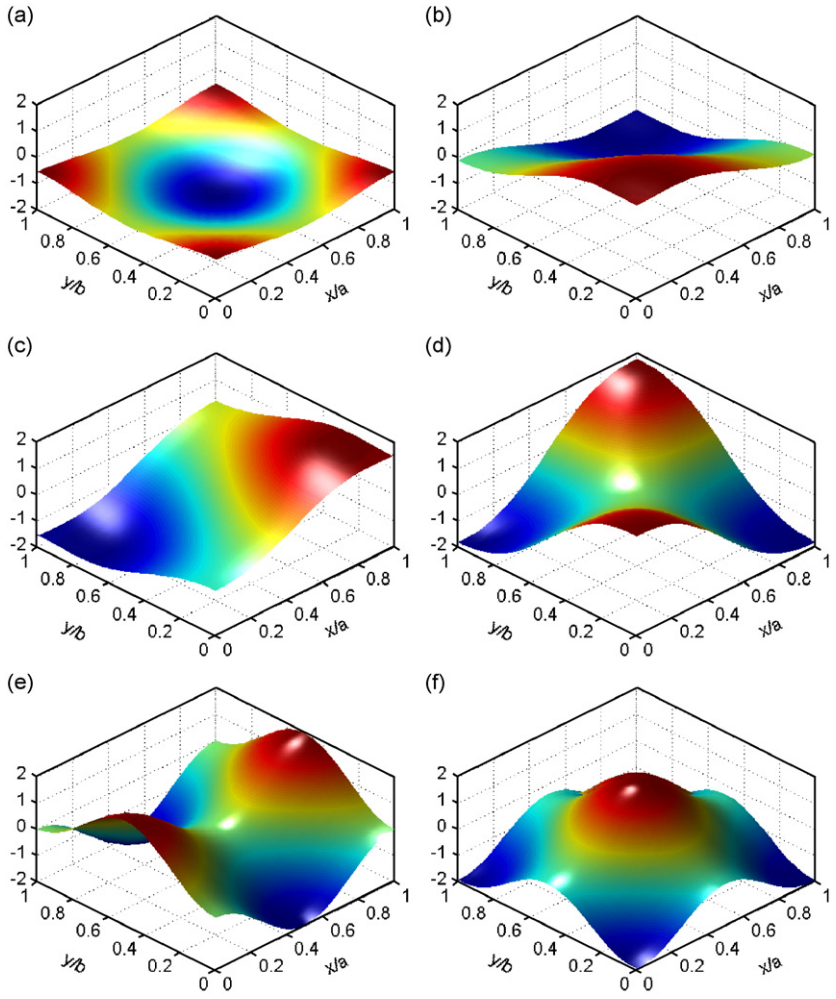

Fig. 2. The mode shapes for square plate with $ka^3/D = 100$, $Ka/D = 1000$ at all four edges. The (a) first, (b) second, (c) third, (d) fourth, (e) fifth, and (f) sixth mode shapes.

one can still see the traces of the modes for a completely clamped plate, the edges and corners now become quite alive in the current case.

4. Conclusions

A general analytical method is proposed for the vibration analysis of a rectangular plate with elastically restrained edges. The displacement solution is here expressed as a combination of several series expansions, and the unknown expansion coefficients are determined from the conditions that both the governing equation and the boundary conditions are satisfied exactly on a point-wise basis. Since each of the series expansions has to be truncated to a finite number of terms in actual numerical calculations, the term "satisfied exactly" should be understood as *satisfied to any specified accuracy*. The current method is universally applicable to a variety of boundary conditions, including all the classical cases. The modification of boundary conditions from one case to another is as simple as modifying the material properties or plate dimensions, and does not involve any change to the solution algorithms or procedures in contrast to most existing methods. Several numerical examples are presented to demonstrate the accuracy and reliability of the proposed solution method. Although this study is focused on plates with uniform elastic supports along an edge, the current method can

be readily extended to other more complicated boundary conditions such as non-uniform elastic restraints, point and partial supports, and their combinations.

Acknowledgments

The first two authors gratefully acknowledge the financial support from NSF Grant CMS-0528263.

Appendix A. Definitions of α_m^l, $\bar{\alpha}_m^l$, $\bar{\bar{\alpha}}_m^l$, β_n^l, $\bar{\beta}_n^l$, and $\bar{\bar{\beta}}_n^l$ used in Eqs. (29)–(31)

Let

$$\xi_a^l(x) = s_1^l \sin\left(\frac{\pi x}{2a}\right) + s_2^l \cos\left(\frac{\pi x}{2a}\right) + s_2^l \sin\left(\frac{3\pi x}{2a}\right) + s_4^l \cos\left(\frac{3\pi x}{2a}\right) \tag{A.1}$$

and

$$\xi_b^l(y) = t_1^l \sin\left(\frac{\pi y}{2a}\right) + t_2^l \cos\left(\frac{\pi y}{2a}\right) + t_2^l \sin\left(\frac{3\pi y}{2a}\right) + t_4^l \cos\left(\frac{3\pi y}{2a}\right). \tag{A.2}$$

Then we define

$$\alpha_m^l = \sum_{p=1}^{4} s_p^l \tau_{am}^p, \quad \bar{\alpha}_m^l = \sum_{p=1}^{4} s_p^l (-\lambda_{ap}^2)\tau_{am}^p, \quad \bar{\bar{\alpha}}_m^l = \sum_{p=1}^{4} s_p^l (\lambda_{ap}^4)\tau_{am}^p, \tag{A.3–A.5}$$

$$\beta_n^l = \sum_{q=1}^{4} t_q^l \kappa_{bn}^q, \quad \bar{\beta}_n^l = \sum_{q=1}^{4} t_q^l (-\lambda_{bq}^2)\kappa_{bn}^q, \quad \text{and} \quad \bar{\bar{\beta}}_n^l = \sum_{q=1}^{4} t_q^l (\lambda_{bq}^4)\kappa_{bn}^q, \tag{A.6–A.8}$$

where τ_{am}^p denote the expansion coefficients of the following functions:

$$\cos\left(\frac{\pi}{2a}x - \frac{\pi}{2}\right) = \sum_{m=0}^{\infty} \tau_{am}^1 \cos\,\lambda_{am}x, \quad \cos\left(\frac{\pi}{2a}x\right) = \sum_{m=0}^{\infty} \tau_{am}^2 \cos\,\lambda_{am}x, \tag{A.9, A.10}$$

$$\cos\left(\frac{3\pi}{2a}x - \frac{\pi}{2}\right) = \sum_{m=0}^{\infty} \tau_{am}^3 \cos\,\lambda_{am}x, \quad \text{and} \quad \cos\left(\frac{3\pi}{2a}x\right) = \sum_{m=0}^{\infty} \tau_{am}^4 \cos\,\lambda_{am}x, \tag{A.11, A.12}$$

and are calculated from

$$\tau_{am}^1 = \begin{cases} m = 0 & \dfrac{2}{\pi} \\ m \neq 0 & \dfrac{4}{(1-4m^2)\pi} \end{cases}, \quad \tau_{am}^2 = \begin{cases} m = 0 & \dfrac{2}{\pi} \\ m \neq 0 & \dfrac{4(-1)^m}{(1-4m^2)\pi} \end{cases}, \tag{A.13, A.14}$$

$$\tau_{am}^3 = \begin{cases} m = 0 & \dfrac{2}{3\pi} \\ m \neq 0 & \dfrac{12}{(9-4m^2)\pi} \end{cases}, \quad \text{and} \quad \tau_{am}^4 = \begin{cases} m = 0 & -\dfrac{2}{3\pi} \\ m \neq 0 & \dfrac{12(-1)^{m+1}}{(9-4m^2)\pi} \end{cases}. \tag{A.15, A.16}$$

The y counterparts, κ_{bn}^q, can be directly obtained from τ_{am}^l by replacing m with n in Eqs. (A.13)–(A.16).

Appendix B. Definitions of H and Q matrixes in Eq. (33)

$$\mathbf{H}=\begin{bmatrix} e_1^1 & e_1^2 & e_1^3 & e_1^4 & f_1^1 & f_1^2 & f_1^3 & f_1^4 \\ e_2^1 & e_2^2 & e_2^3 & e_2^4 & f_2^1 & f_2^2 & f_2^3 & f_2^4 \\ e_3^1 & e_3^2 & e_3^3 & e_3^4 & f_3^1 & f_3^2 & f_3^3 & f_3^4 \\ e_4^1 & e_4^2 & e_4^3 & e_4^4 & f_4^1 & f_4^2 & f_4^3 & f_4^4 \\ e_5^1 & e_5^2 & e_5^3 & e_5^4 & f_5^1 & f_5^2 & f_5^3 & f_5^4 \\ e_6^1 & e_6^2 & e_6^3 & e_6^4 & f_6^1 & f_6^2 & f_6^3 & f_6^4 \\ e_7^1 & e_7^2 & e_7^3 & e_7^4 & f_7^1 & f_7^2 & f_7^3 & f_7^4 \\ e_8^1 & e_8^2 & e_8^3 & e_8^4 & f_8^1 & f_8^2 & f_8^3 & f_8^4 \end{bmatrix}, \tag{B.1}$$

where

$$e^l_{1n,m}=\frac{k_{x0}}{D}\beta^l_n,\quad f^l_{1n,n}=\frac{k_{x0}}{D}\xi^l_a(0)-\delta_{l1}(2-v)\lambda^2_{bn}+\delta_{l3}, \tag{B.2, B.3}$$

$$e^l_{2n,m}=-\lambda^2_{am}\beta^l_n+v\bar{\beta}^l_n,\quad f^l_{2n,n}=\xi''^l_a(0)+v(-\lambda^2_{bn})\xi^l_a(0)-\delta_{l1}\frac{K_{x0}}{D}, \tag{B.4, B.5}$$

$$e^l_{3n,m}=\frac{k_{xa}}{D}\beta^l_n(-1)^m,\quad f^l_{3n,n}=\frac{k_{xa}}{D}\xi^l_a(a)+\delta_{l2}(2-v)\lambda^2_{bn}-\delta_{l4}, \tag{B.6, B.7}$$

$$e^l_{4n,m}=(-1)^m[-\lambda^2_{am}\beta^l_n+v\bar{\beta}^l_n],\quad f^l_{4n,n}=\xi''^l_a(a)+v(-\lambda^2_{bn})\xi^l_a(a)+\delta_{l2}\frac{K_{xa}}{D}, \tag{B.8, B.9}$$

$$f^l_{5m,n}=\frac{k_{y0}}{D}\alpha^l_m,\quad e^l_{5m,m}=\frac{k_{y0}}{D}\xi^l_b(0)-\delta_{l1}(2-v)\lambda^2_{am}+\delta_{l3}, \tag{B.10, B.11}$$

$$f^l_{6m,n}=-\lambda^2_{bn}\alpha^l_m+v\bar{\alpha}^l_m,\quad e^l_{6m,m}=\xi''^l_b(0)+v(-\lambda^2_{am})\xi^l_b(0)-\delta_{l1}\frac{K_{y0}}{D}, \tag{B.12, B.13}$$

$$f^l_{7m,n}=\frac{k_{yb}}{D}\alpha^l_m(-1)^n,\quad e^l_{7m,m}=\frac{k_{yb}}{D}\xi^l_b(b)+\delta_{l2}(2-v)\lambda^2_{am}-\delta_{l4}, \tag{B.14, B.15}$$

$$f^l_{8m,n}=(-1)^n[-\lambda^2_{bn}\alpha^l_m+v\bar{\alpha}^l_m],\quad \text{and}\quad e^l_{8m,m}=\xi''^l_b(b)+v(-\lambda^2_{am})\xi^l_b(b)+\delta_{l2}\frac{K_{yb}}{D}. \tag{B.16, B.17}$$

$$\mathbf{Q}=\begin{bmatrix}\mathbf{Q}_1 & \mathbf{Q}_2 & \mathbf{Q}_3 & \mathbf{Q}_4 & \mathbf{Q}_5 & \mathbf{Q}_6 & \mathbf{Q}_7 & \mathbf{Q}_8\end{bmatrix}^{\mathrm{T}}, \tag{B.18}$$

where

$$Q_{1n,p}=\frac{-k_{x0}}{D},\quad Q_{2n,p}=\lambda^2_{am}+v\lambda^2_{bn},\quad Q_{3n,p}=\frac{k_{xa}}{D}(-1)^{m+1}, \tag{B.19−B.21}$$

$$Q_{4n,p}=(-1)^m[\lambda^2_{am}+v\lambda^2_{bn}],\quad Q_{5m,p}=\frac{-k_{y0}}{D},\quad Q_{6m,p}=\lambda^2_{bn}+v\lambda^2_{am}, \tag{B.22−B.24}$$

$$Q_{7m,p}=\frac{k_{yb}}{D}(-1)^{n+1},\quad \text{and}\quad Q_{8m,p}=(-1)^n[\lambda^2_{bn}+v\lambda^2_{am}]\quad (p=nM+m). \tag{B.25, B.26}$$

Appendix C. Definitions of matrices in Eq. (36)

$\tilde{\mathbf{K}}$ and $\tilde{\mathbf{M}}$ are diagonal matrices. Their elements are defined as

$$\tilde{K}_{nM+m,nM+m} = \lambda_{am}^4 + \lambda_{bn}^4 + 2\lambda_{am}^2\lambda_{bn}^2 \quad \text{and} \quad \tilde{M}_{nM+m,nM+m} = 1. \tag{C.1, C.2}$$

$$\mathbf{B} = \begin{bmatrix} \mathbf{B}_a^1 & \mathbf{B}_a^2 & \mathbf{B}_a^3 & \mathbf{B}_a^4 & \mathbf{B}_b^1 & \mathbf{B}_b^2 & \mathbf{B}_b^3 & \mathbf{B}_b^4 \end{bmatrix}, \tag{C.3}$$

where

$$B_{ap,m}^l = \lambda_{am}^4\beta_n^l + \bar{\bar{\beta}}_n^l - 2\lambda_{am}^2\bar{\beta}_n^l, \quad B_{bp,n}^l = \lambda_{bn}^4\alpha_m^l + \bar{\bar{\alpha}}_m^l - 2\lambda_{bn}^2\bar{\alpha}_m^l. \tag{C.4, C.5}$$

$$\mathbf{F} = \begin{bmatrix} \mathbf{F}_a^1 & \mathbf{F}_a^2 & \mathbf{F}_a^3 & \mathbf{F}_a^4 & \mathbf{F}_b^1 & \mathbf{F}_b^2 & \mathbf{F}_b^3 & \mathbf{F}_b^4 \end{bmatrix}, \tag{C.6}$$

where

$$F_{ap,m}^l = \beta_n^l \quad \text{and} \quad F_{bp,n}^l = \alpha_m^l \quad (p = nM + m). \tag{C.7, C.8}$$

References

[1] A.W. Leissa, *Vibration of Plates*, Acoustical Society of America, 1993.

[2] G.B. Warburton, The vibrations of rectangular plates, *Proceeding of the Institute of Mechanical Engineers, Series A* 168 (1954) 371–384.

[3] A.W. Leissa, The free vibrations of rectangular plates, *Journal of Sound and Vibration* 31 (1973) 257–293.

[4] S.M. Dickinson, E.K.H. Li, On the use of simply supported plate functions in the Rayleigh–Ritz method applied to the vibration of rectangular plates, *Journal of Sound and Vibration* 80 (1982) 292–297.

[5] G.B. Warburton, Response using the Rayleigh–Ritz method, *Journal of Earthquake Engineering and Structural Dynamics* 7 (1979) 327–334.

[6] G.B. Warburton, S.L. Edney, Vibrations of rectangular plates with elastically restrained edges, *Journal of Sound and Vibration* 95 (1984) 537–552.

[7] P.A.A. Laura, R.O.G. Grossi, Transverse vibration of rectangular plates with edges elastically restrained against translation and rotation, *Journal of Sound and Vibration* 75 (1981) 101–107.

[8] P. Cupial, Calculation of the natural frequencies of composite plates by the Rayleigh–Ritz method with orthogonal polynomials, *Journal of Sound and Vibration* 201 (1997) 385–387.

[9] R.B. Bhat, Natural frequencies of rectangular plates using characteristic orthogonal polynomials in the Rayleigh–Ritz method, *Journal of Applied Mechanics* 102 (1985) 493–499.

[10] S.M. Dickinson, A. Di-Blasio, On the use of orthogonal polynomials in the Rayleigh–Ritz method for the flexural vibration and buckling of isotropic and orthotropic rectangular plates, *Journal of Applied Mechanics* 108 (1986) 51–62.

[11] P.A.A. Laura, Comments on "Natural frequencies of rectangular plates using a set of static beam functions in the Rayleigh–Ritz method," *Journal of Sound and Vibration* 200 (1997) 540–542.

[12] D. Zhou, Natural frequencies of elastically restrained rectangular plates using a set of static beam functions in the Rayleigh–Ritz method, *Computers and Structures* 57 (1995) 731–735.

[13] D. Zhou, Natural frequencies of rectangular plates using a set of static beam functions in the Rayleigh–Ritz method, *Journal of Sound and Vibration* 189 (1996) 81–88.

[14] W.L. Li, M. Daniels, A Fourier series method for the vibrations of elastically restrained plates arbitrarily loaded with springs and masses, *Journal of Sound and Vibration* 252 (2002) 768–781.

[15] O. Beslin, J. Nicolas, A hierarchical functions sets for very high-order plate bending modes with any boundary conditions, *Journal of Sound and Vibration* 202 (1997) 633–655.

[16] W.L. Li, Vibration analysis of rectangular plates with general elastic boundary supports, *Journal of Sound and Vibration* 273 (2004) 619–635.

[17] D.J. Gorman, A comprehensive study of the free vibration of rectangular plates resting on symmetrically-distributed uniform elastic edge supports, *Journal of Applied Mechanics* 56 (1980) 893–899.

[18] D.J. Gorman, Free vibration and buckling of in-plane loaded plates with rotational elastic edge support, *Journal of Sound and Vibration* 225 (2000) 755–773.

[19] D.J. Gorman, Free vibration analysis of corner-supported rectangular plates with symmetrically distributed edge beams, *Journal of Sound and Vibration* 263 (2003) 979–1003.

[20] D.J. Gorman, Free vibration analysis of Mindlin plates with uniform elastic edge support by the superposition method, *Journal of Sound and Vibration* 207 (1997) 335–350.
[21] S. Hurlebaus, L. Gaul, J.T.-S. Wang, An exact solution for calculating the eigenfrequencies of orthotropic plates with completely free boundary, *Journal of Sound and Vibration* 244 (2001) 747–759.
[22] M.B. Rosales, C.P. Filipich, Vibration of orthotropic plates: discussion on the completeness of the solutions used in direct methods, *Journal of Sound and Vibration* 261 (2003) 751–757.
[23] C.P. Filipich, M.B. Rosales, Arbitrary precision frequencies of a free rectangular thin plate, *Journal of Sound and Vibration* 230 (2000) 521–539.
[24] W.L. Li, Free vibration of beams with general boundary conditions, *Journal of Sound and Vibration* 237 (2000) 709–725.
[25] J.T. Du, W.L. Li, G.Y. Jin, T.J. Yang, Z.G. Liu, An analytical method for the in-plane vibration analysis of rectangular plates with elastically restrained edges, *Journal of Sound and Vibration* 306 (2007) 908–927.